

Supporting Information

Large-Scale Synthesis of $\text{Co}_2\text{V}_2\text{O}_7$ Hexagonal Microplatelets under Ambient Conditions for Highly Reversible Lithium Storage

Fangfang Wu,^a Chunhui Yu,^a Wenxiu Liu,^a Ting Wang,^a Jinkui Feng,^a and Shenglin Xiong^{,a}*

^aKey Laboratory of the Colloid and Interface Chemistry, Ministry of Education, and School of Chemistry and Chemical Engineering, Shandong University, Jinan, 250100, PR China

E-mail: chexsl@sdu.edu.cn (S. L. X.)

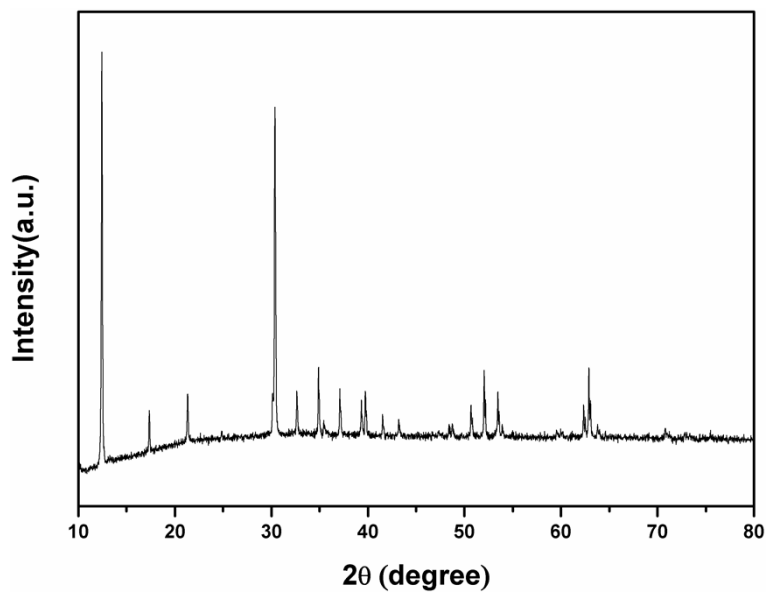


Figure S1. XRD patterns of the product obtained after the low temperature water bath.

Table S1. Summary of diffraction peak position calculated and observed.

h	k	l	2θ(cal)	2θ(obs)	$\Delta 2\theta^{\#}$	d(cal)	d(obs)	$\Delta d^{\#}$
0	1	0	12.241	12.409	0.037	7.2247	7.1269	-0.0209
1	0	0	17.275	17.355	0.125	5.1289	5.1054	-0.0363
0	1	1	21.113	21.331	-0.013	4.2045	4.162	0.0025
0	2	0	24.624	24.834	-0.005	3.6124	3.5823	0.0007
-1	0	2	30.147	30.127	0.226	2.9619	2.9639	-0.0216
0	2	1	30.155	30.363	-0.003	2.9612	2.9414	0.0002
1	1	1	32.429	32.628	0.006	2.7586	2.7422	-0.0005
0	0	2	34.671	34.883	-0.007	2.5851	2.5699	0.0005
-2	0	2	35.233	35.434	0.004	2.5452	2.5312	-0.0003
0	1	2	36.899	37.094	0.01	2.434	2.4217	-0.0006
1	2	1	39.117	39.315	0.008	2.3009	2.2898	-0.0005
-2	2	1	39.499	39.728	-0.024	2.2796	2.2669	0.0013
0	3	1	41.323	41.52	0.008	2.183	2.1731	-0.0004
0	2	2	42.988	43.204	-0.011	2.1023	2.0923	0.0005
1	1	2	48.15	48.417	-0.061	1.8882	1.8785	0.0022
1	3	1	48.534	48.751	-0.012	1.8742	1.8664	0.0004
0	4	0	50.487	50.682	0.01	1.8062	1.7997	-0.0003
0	3	2	51.843	52.039	0.009	1.7621	1.7559	-0.0003
1	2	2	53.204	53.451	-0.042	1.7202	1.7128	0.0013
0	4	1	53.711	53.913	0.003	1.7051	1.6992	-0.0001
2	0	2	62.15	62.333	0.021	1.4923	1.4884	-0.0005
-2	0	4	62.681	62.883	0.004	1.481	1.4767	-0.0001
1	2	3	70.53	70.788	-0.053	1.3341	1.3299	0.0009

$\# \Delta 2\theta = 2\theta(\text{obs}) - 2\theta(\text{cal})$ $\Delta d = d(\text{obs}) - d(\text{cal})$

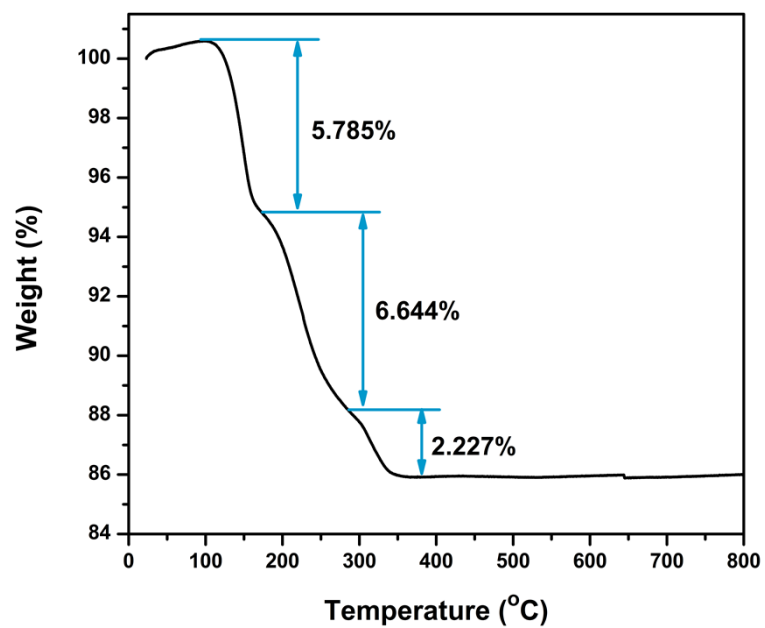


Figure S3. TGA curve of $\text{Co}_2\text{V}_2\text{O}_7 \cdot n\text{H}_2\text{O}$ MNHPs at laboratory air.

Table S3. The ratio of $\text{Co}^{2+}/\text{Co}^{3+}$ and $\text{V}^{4+}/\text{V}^{5+}$ in the products based on the total areas of peaks after a Gaussian fitting method.

Composite	Total areas of fitted peaks	The ratio of $\text{Co}^{2+}/\text{Co}^{3+}$ and $\text{V}^{4+}/\text{V}^{5+}$
Co^{2+}	12724.004	2.03
Co^{3+}	6279.338	
V^{4+}	2781.5151	0.79
V^{5+}	3511.3894	

NOTE: As shown in Table S1, the ratio of $\text{Co}^{2+}/\text{Co}^{3+}$ and $\text{V}^{4+}/\text{V}^{5+}$ are 2.03 and 0.79, respectively. The cationic V^{4+} exists in $\text{Co}_2\text{V}_2\text{O}_7$, which is likely due to non-completely reduced oxygen, coincided with previous literature reported.^{1,2} This phenomenon of Co^{3+} and Co^{2+} coexisting on surface of $\text{Co}_2\text{V}_2\text{O}_7$ is common in TMOs, such as NiCo_2O_4 with Co^{2+} , Co^{3+} , Ni^{2+} and Ni^{3+} co-existing on the surface.³⁻⁶ The formation of Co^{3+} can be assigned to be oxidized by oxygen when exposed to air.⁷

(1) A. J. Xu, Q. Lin, M. J. Jia, B. Zhaorigetu, *React. Kinet. Catal. Lett.* **2008**, 93, 273-280.

(2) S. R. G. Carrazan, C. Peres, J. P. Bernard, M. Ruwet, P. Ruiz, B. Delmon, *J. Catal.* **1996**, 158, 452-476.

(3) C. Z. Yuan, J. Y. Li, L. R. Hou, X. G. Zhang, L. F. Shen, X. W. Lou, *Adv. Funct. Mater.* **2012**, 22, 1592-1597.

(4) L. F. Shen, Q. Che, H. S. Li, X. G. Zhang, *Adv. Funct. Mater.* **2012**, 24, 2630-2637.

(5) J. F. Li, S. L. Xiong, Y. R. Liu, Z. C. Ju, Y. T. Qian, *ACS Appl. Mater. Interfaces* 2013,5,981-988.

(6) A. Thissen, D. Enslin, F.J. Fernandez-Madrigal, W. Jaegermann, R. Alcantara, P. Lavela, J. L. Tirado, *Chem. Mater.* **2005**, 17, 5202-5208.

(7) D. Gazzoli, M. Occhiuzzi, A. Cimino, D. Cordischi, G. Minelli, Fulvia Pinzari, *J. Chem. Soc., Faraday Trans.*, **1996**, 92, 4567-4574.

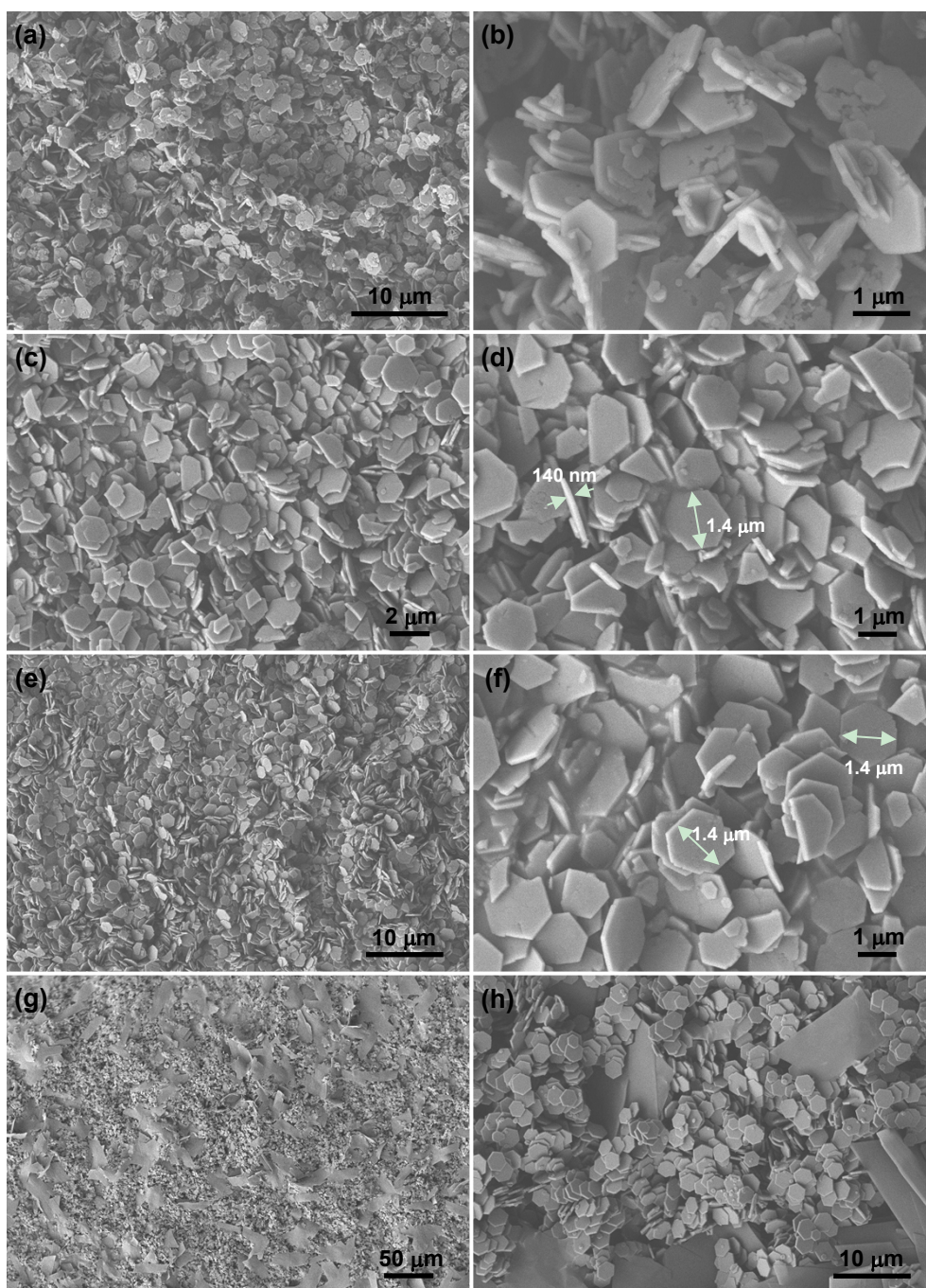


Figure S4. Typical FESEM images of the samples: a,b) prepared in the presence of 1 mmol HMT (0.025 mol/L), c,d) prepared in the presence of 2 mmol HMT (0.05 mol/L), e,f) prepared in the presence of 3 mmol HMT (0.075 mol/L), g,h) prepared in the presence of 10 mmol HMT (0.25 mol/L), with the other conditions kept the same.

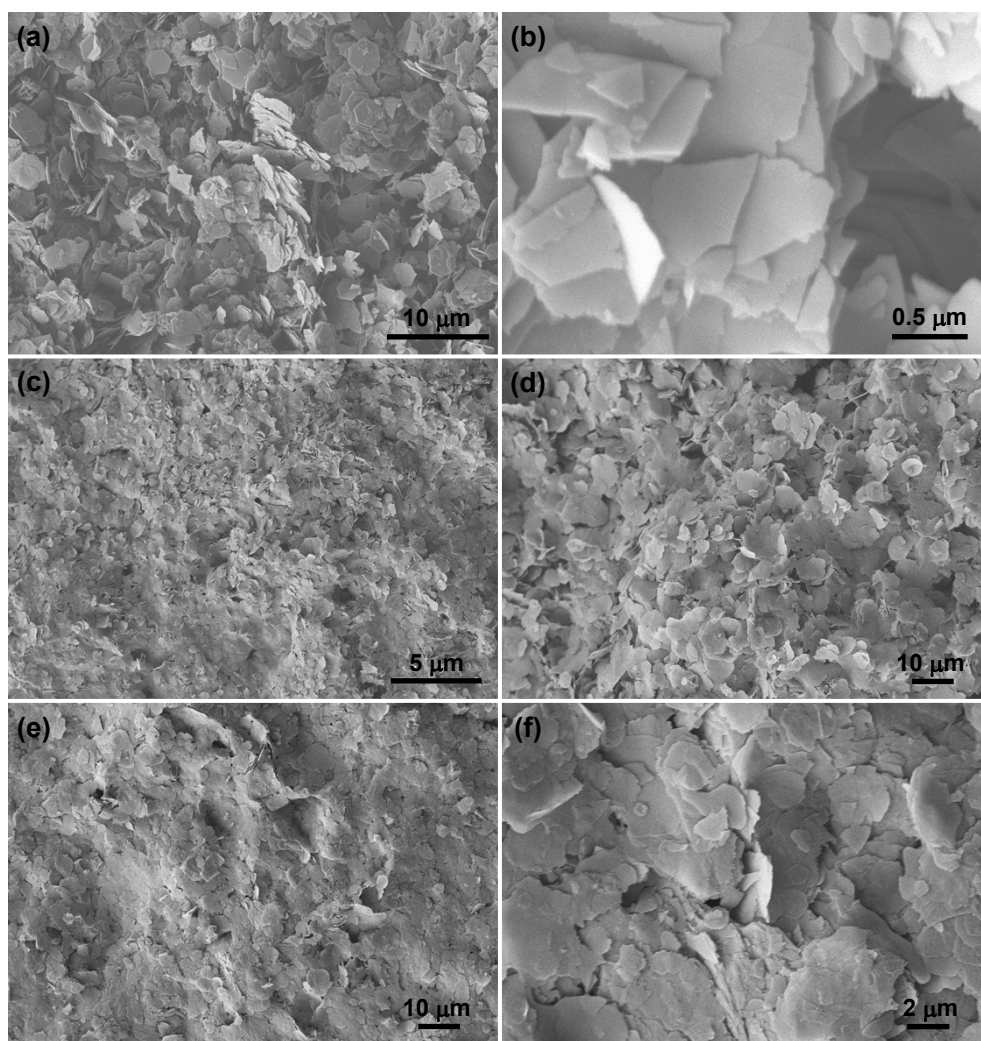


Figure S5. Typical FESEM images of the samples: a,b) prepared by replacing HMT with 1.25 mmol NaOH, c,d) prepared by replacing HMT with 1.5 mmol NaOH, e,f) prepared by replacing NaOH with 1.6 mmol KOH, g,h) prepared by replacing HMT with 2 mmol NaOH, with the other conditions kept the same.

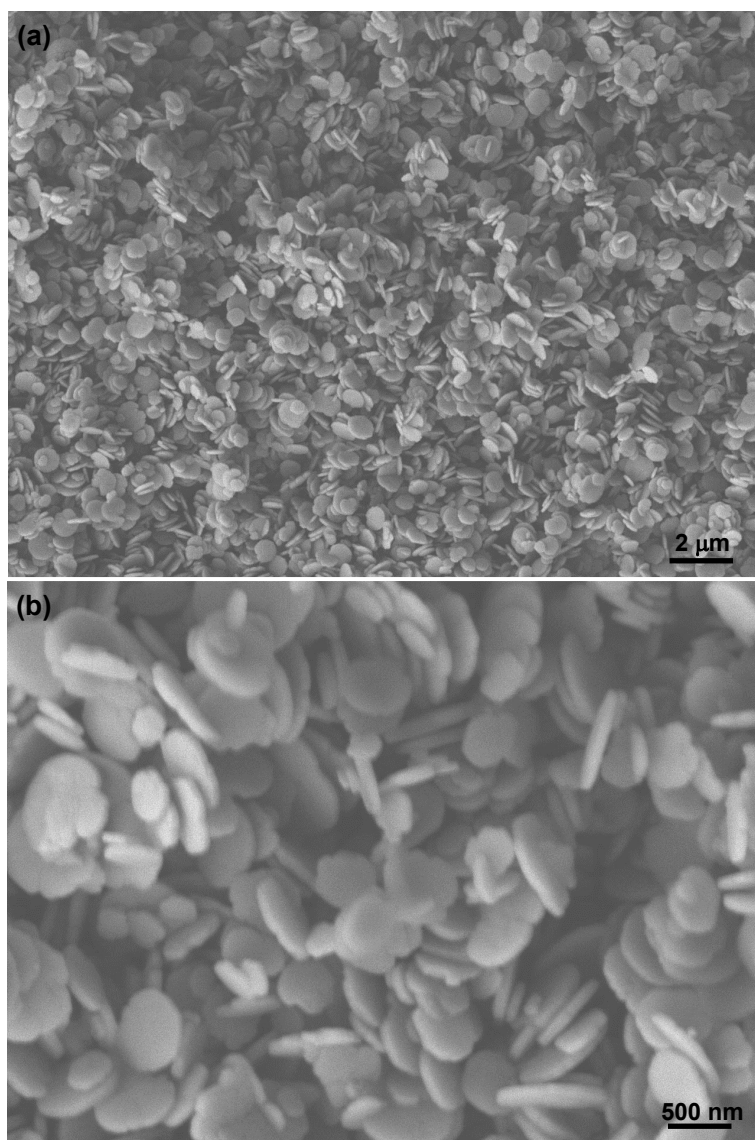


Figure S6. Typical FESEM images of the samples prepared when the water bath temperature is 60 °C, with the other conditions kept the same.

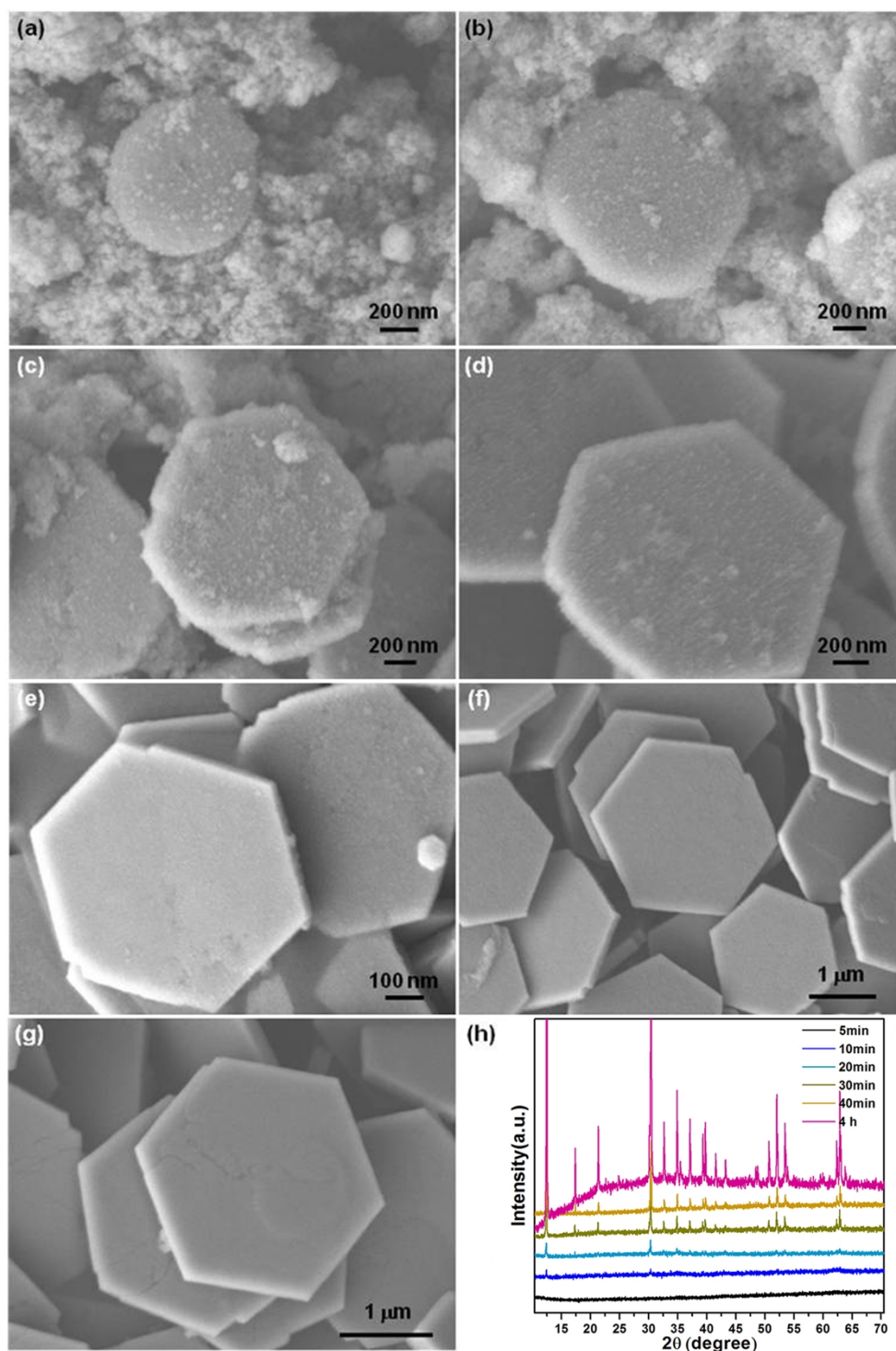


Figure S7. Structural evolution of $\text{Co}_2\text{V}_2\text{O}_7 \cdot n\text{H}_2\text{O}$ MNPs prepared at 80 °C water bath with different reaction times (FESEM images): 5 min (a), 10 min (b), 20 min (c), 30 min (d), 40 min (e), 60 min (f) and 240 min (g). (h) XRD pattern of the $\text{Co}_2\text{V}_2\text{O}_7 \cdot n\text{H}_2\text{O}$ obtained at different reaction time.

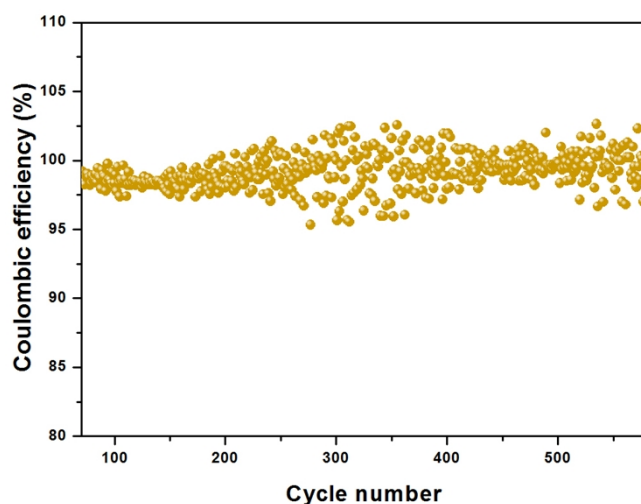


Figure S8. The enlarged CE range from 80% to 110% of the Figure 7f.

NOTE: We think the CE data above 100% is due to the slightly variation of temperature during cycling. For example, when the temperature is low, the lithium diffusion rate is limited and lithium cannot be fully extracted, the CE is less than 100%, when temperature is high, the excess lithium is extracted, the CE is higher than 100%.

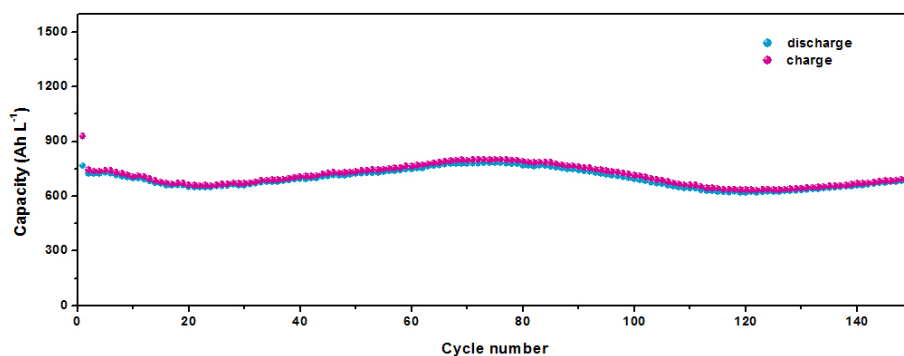


Figure S9. Volumetric capacities of porous $\text{Co}_2\text{V}_2\text{O}_7$ MHNPs electrode materials at a current density of 400 mA cm^{-3} .

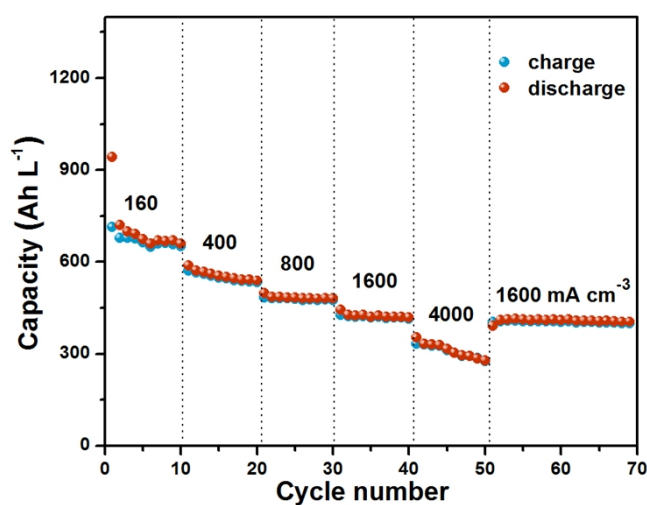


Figure S10. Volumetric capacities of porous $\text{Co}_2\text{V}_2\text{O}_7$ MHNPs electrode materials at different current densities.

(The volumetric capacity (C_v) of the electrode is calculated as follows:[¹]

$$C_v (\text{mAh cm}^{-3}) = C_g (\text{mAh g}^{-1}) \times \rho (\text{g cm}^{-3})$$

Note: C_g and ρ are the specific capacity and tap density of electrochemically active material, respectively.

[1] B. Wang, X. L. Li, T. F. Qiu, B. Luo, J. Ning, J. Li, X. F. Zhang, M. H. Liang, L. J. Zhi, *Nano Lett.* **2013**, *13*, 5578-5584.

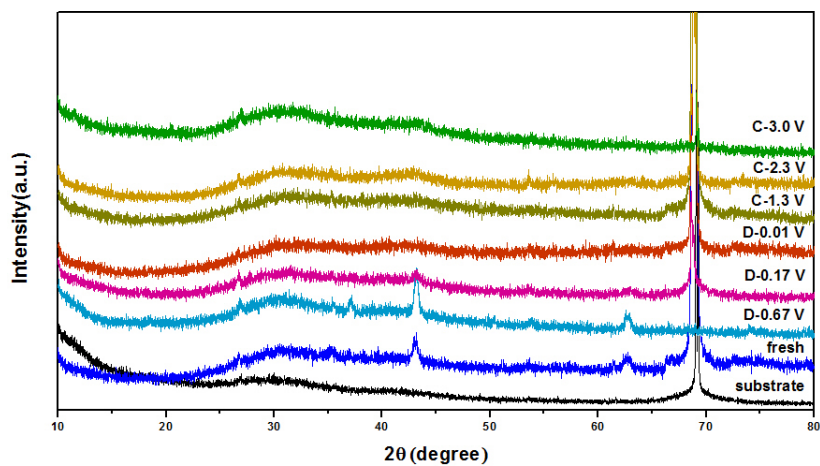


Figure S11. Ex-situ XRD patterns of the electrode materials under different discharge and charge state.

Note: fresh = pristine electrode materials, substrate = Si substrate.

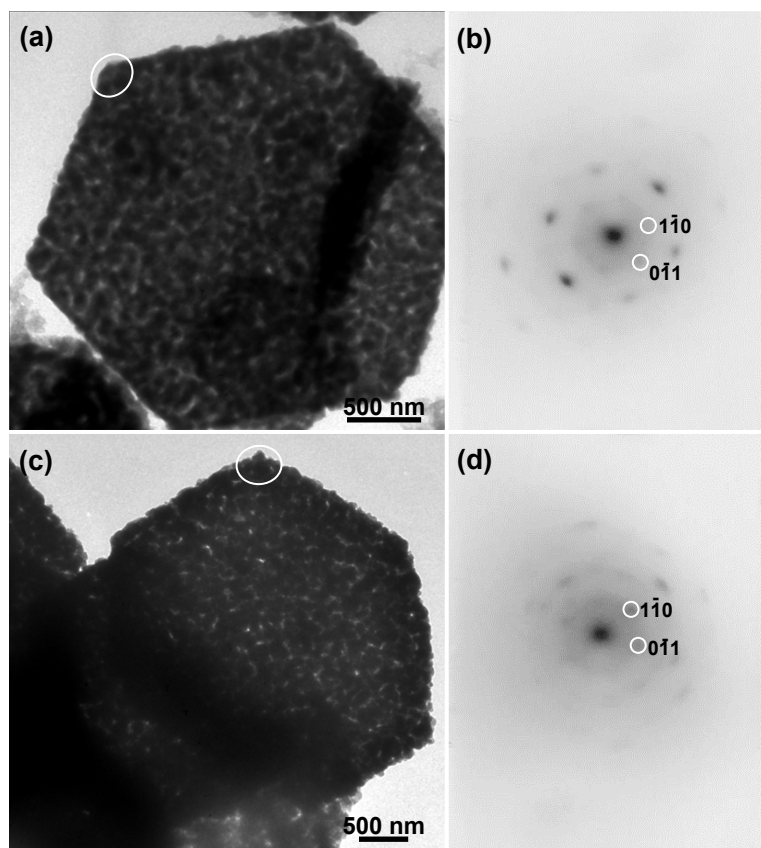


Figure S12. Ex-situ TEM images and the corresponding SAED pattern of electrode material at fully-discharged 0.01 V (a,b) and -charged 3.0 V (c,d).

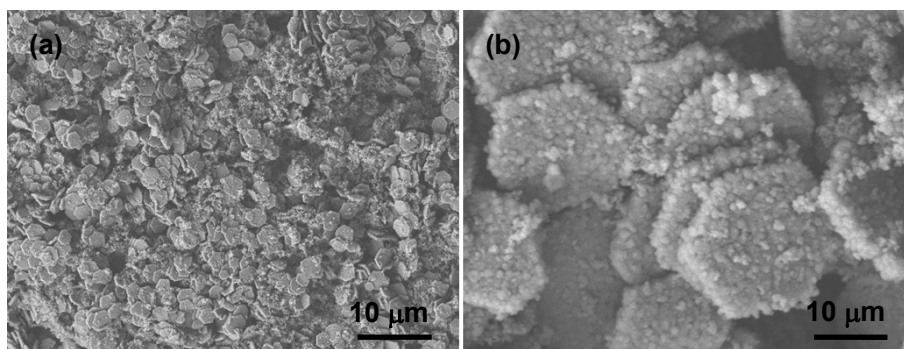


Figure S13. The FESEM images of the $\text{Co}_2\text{V}_2\text{O}_7$ anode materials after 50 cycles at the current density of 1 A g^{-1} .